



## Porous Polyvinyl Formaldehyde / MWCNTs Foam for Pb<sup>+2</sup> Removal from Water

Mohammed Yosef<sup>1</sup>; Alaa Fahmy<sup>1</sup>; Ali Hassan<sup>1</sup>; Walid Mosaad El Hotaby<sup>2</sup>; Badawi Anis<sup>2</sup>



CrossMark

<sup>1</sup>Chemistry Department, Faculty of Science, Al Azhar University, 11884 Cairo, Egypt

<sup>2</sup>Spectroscopy Department., Physics Division., National Research Centre, Dokki, Giza, Egypt

### Abstract

Preparation of macro-porous polyvinyl formaldehyde / multi-walled carbon nanotubes (PVF/MWCNTs) foam was done via one step reaction during acetalization of polyvinyl alcohol (PVA). The as-prepared PVF/MWCNTs composite was used as an eco-friendly, easy recovery sorbents for Pb (II) from aqueous medium. Fourier transform infrared (FTIR), and high-resolution scanning electron microscopy (HRSEM) were used to investigate the chemical composition and morphological structure of the prepared foam. The results showed that equilibrium occurred within 60 min at pH $\approx$  5 with a maximum adsorption capacity 3.4 mg/g with 43 % removal (considering the total weight of composite). In addition, the kinetic results are most fitted with pseudo-second-order model indicating that the reaction mechanism is chemisorption in nature. Therefore, it is suggested that the prepared PVF/MWCNTs foam can be used in water treatment systems as an eco-friendly and efficiency sorbent.

**Keywords:** MWCNTs; adsorption kinetics; heavy metal removal; water treatment

### 1.Introduction

Contamination of aquatic system by hazardous pollutants such as heavy metals has become a great threat to human health. Unfortunately, heavy metal ions are not biodegradable and proved to be accumulated in the body causing many diseases [1–3]. Among them, as non-biodegradable pollutant, lead can be considered as one of the most poisonous heavy metal which poses a direct threat for both humans and animals by accumulating in the living tissues throughout the food chains causing serious health problems [4,5]. Thus, removal of heavy metals from contaminated aqueous mediums has become very essential process. Therefore, various techniques have been reported for the removal of poisonous heavy metals from polluted aquatic sources such as; ion-exchange, reverse osmosis, chemical coagulation, solvent extraction, and adsorption [6–9]. Adsorption technique is considered to be one of the most conventional, economical, and efficient technique which applied to

metal ions removal from aqueous mediums [10,11]. Many adsorbents have been used in treatment processes, such as polymers [12], activated carbon [13], graphene oxide [14], and resins [15]. According to its unique structure, physical, and chemical properties many studies have been reported on using multi-walled carbon nanotubes (MWCNTs) as efficient adsorbents for removing lead ions from aqueous solutions. Li *et al.*, reported that refluxing as-grown MWCNTs with concentrated nitric acid increased the maximum adsorption capacity ( $Q_t$ ) from 1 mg/g to 15.6 mg/g [16]. Oxidized MWCNTs exhibited  $Q_t$  value of 4.09 mg/g [17]. Chemically modified MWCNTs with 3-hydroxy-4-((3-silylpropylimino) methyl) phenol showed a maximum  $Q_t$  of 36.8 mg/g at pH= 4 [18]. MWCNTs functionalized by glutaric dihydrazide (GDH) showed  $Q_t$  of 22.1, mg/g at pH 4.0 [19]. MWCNTs modified with pyridine group showed  $Q_t$  of 179 mg/g for Pb ions removal [20]. Jahangiri *et al.*, showed that MWCNTs modified with 1-isatin-3-

\*Corresponding author e-mail: [badawi.ali@daad-alumni.de](mailto:badawi.ali@daad-alumni.de)

Receive Date: 09 July 2020, Revise Date: 13 August 2020, Accept Date: 16 August 2020

DOI: 10.21608/EJCHEM.2020.34453.2733

©2021 National Information and Documentation Center (NIDOC)

thiosemicarbazone had a maximum  $Q_t$  value of 14.56 mg/g [21].

However, there are serious health and environmental risks upon releasing MWCNTs into aquatic systems. So, sophisticated process such as high centrifugation or ultra-filtration is needed to remove MWCNTs powder from treated water before releasing it into the environment [22]. Therefore, environmentally safe sorbents are needed to avoid the risk of MWCNTs leakage into water [23].

In the present study, immobilization of MWCNTs powder into an open cell polyvinyl formaldehyde (PVF) foam matrix was made by one step acetylation reaction method. The as prepared PVF/MWCNTs foam suggested to be used as an effective easy recovery sorbent for Pb ions removal from aqueous solutions. Sorption experiments and kinetic studies were performed to study the removal efficiency and sorption mechanisms of the prepared PVF/MWCNTs foam.

## 2. Experimental

### 2.1. Materials

Hydrolyzed polyvinyl alcohol (PVA) 98–99% high molecular weight and formaldehyde were bought from Alfa Aesar (Germany). Hydrochloric acid (37%, HCl), nitric acid (70%, HNO<sub>3</sub>), and sulfuric acid (98%, H<sub>2</sub>SO<sub>4</sub>), were purchased from Fischer scientific (Germany). Magnesium nitrate Mg(NO<sub>3</sub>)<sub>2</sub>·6H<sub>2</sub>O (99.00%), ferric nitrate Fe(NO<sub>3</sub>)<sub>3</sub>·9H<sub>2</sub>O (99.99%), ammonium molybdate hydrate (NH<sub>4</sub>)<sub>6</sub>Mo<sub>7</sub>O<sub>24</sub>·4H<sub>2</sub>O (99.98%), and urea (99.00%) were bought from Sigma–Aldrich (Germany). Lead nitrate (analytical grade) was purchased from Merck (Germany). Milli Q distilled – de ionized water was used during this study. No further purification was made for the chemicals.

### 2.2. Synthesis of multiwall carbon nanotubes (MWCNTs)

Preparation of multi-walled carbon nanotubes was carried out with in-house-assembled chemical vapor deposition technique (CVD) setup. Combustion route was used to prepare nanoparticles of Fe and Mo supported over magnesium oxide (MgO) catalyst. The Mo:Fe:MgO molar ratio was kept at 1:1:13 [24][25]. The catalyst then spread uniformly over a quartz boat and inserted into a quartz tube inside an electrical tube furnace heated to

700 °C in hydrogen atmosphere (1000 sscm). Subsequently, acetylene (50 sscm) gas was introduced into the reactor for 30 min. The resulted black dense material containing MWCNTs around the oxide grains was carefully ground to a fine powder. The as-prepared MWCNTs were refluxed at 60 °C for 24 h with concentrated hydrochloric acid (HCl) then washed several times with de-ionized water to neutralize and remove the acid traces. After that, the product was dried and then dispersed in ethanol under sonication and filtered using cellulose nitrate filter paper (0.2 µm). The filtered product then dried at 100 °C for 6 h under dynamic vacuum.

### 2.3. Preparation of PVF, PVF/MWCNTs foams

PVF foam was prepared as reported in literature [25][26]. Briefly, 10 wt % of PVA solution was prepared by dissolving 5 g PVA powder in 45 ml deionized water during magnetic stirring at 90 °C for complete dissolution of PVA. 10 mL of formaldehyde were added to the prepared solution. Then, 30 mL of 50 wt% H<sub>2</sub>SO<sub>4</sub> was added to the prepared froth at room temperature [25]. Finally, the obtained froth was baked at 60 °C for about 6 hours in an oven. To remove the un-reacted materials, the resulted foam sample was washed with deionized water many times and dried at 60 °C. The prepared pure PVF foam is shown in Fig.1 (a)

*In-situ* method was employed to prepare PVF/MWCNTs foam. Typically, 50 mg of prepared MWCNTs was sonicated for 30 min in 15 mL deionized water. The resulted solution was added to the PVA solution during vigorously stirring before the addition of formaldehyde. The foaming process continued as explained above. The color of the PVF/MWCNTs foam obviously changed from white to homogenous black indicating a homogenous distribution of MWCNTs inside PVF matrix. The prepared PVF/MWCNTs foam is presented in Fig.1 (b). For adsorption experiments, the PVF/MWCNTs foam was cut into small pieces to increase the active surface and then refluxed with 10% sulfuric acid at 60 °C for 24 h to increase the amount of oxygenated functional groups over the surface, then washed again and finally dried at 60 °C in an oven for 1h [Fig. 1(c) and (d)].

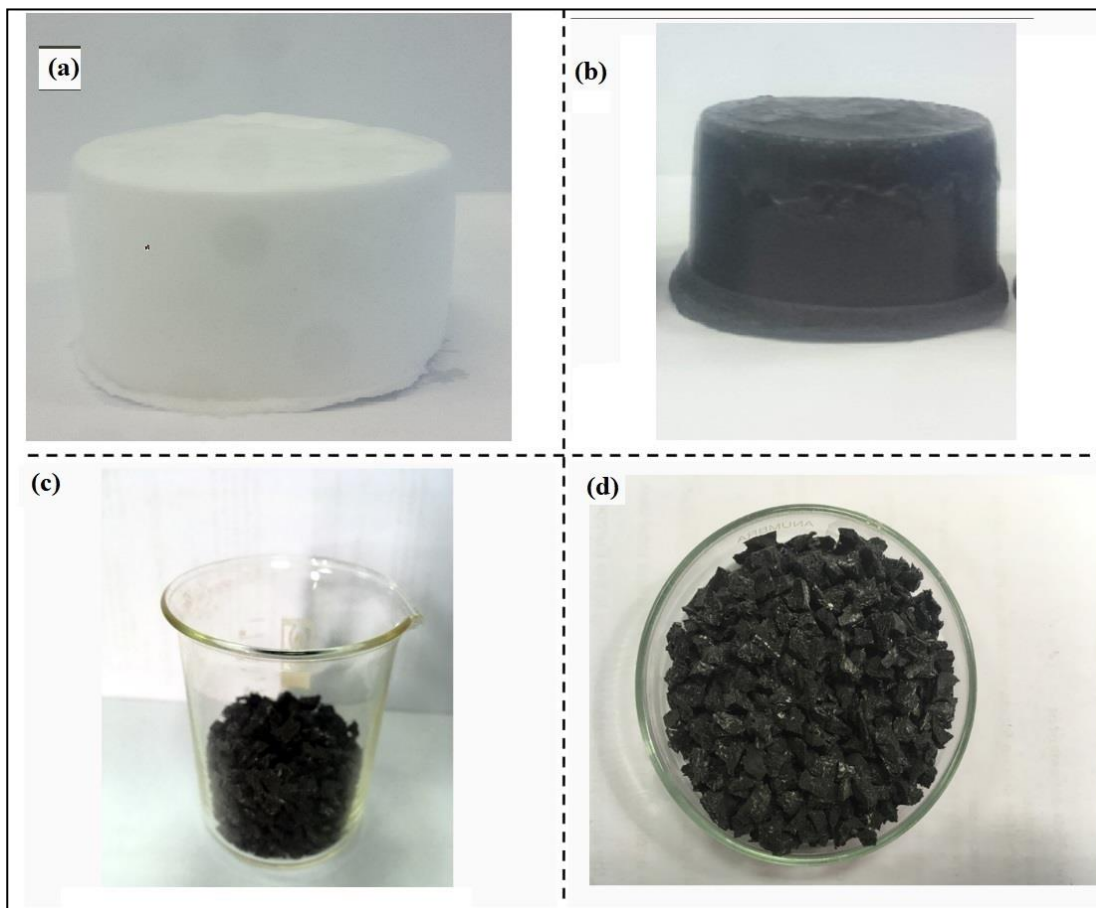


Figure 1: Optical images of (a) as prepared pure PVF foams, (b) PVF/MWCNTs foam, (c) washing of the small pieces of PVF/MWCNTs to remove any reactant residuals, and (d) dried PVF/MWCNTs foam pieces.

#### 2.4. Preparation of Pb (II) stock solution

1000 mg/L of Pb (II) stock solution was prepared by dissolving lead nitrate in deionized water. Then, further dilution by deionized water to the desired concentrations for the conducted experiments.

#### 2.5. Batch experiments

It is well known that the adsorption capacity is highly dependent on the pH value of the solution. To study the effect of pH, 0.04 g of the prepared PVF and PVF/MWCNTs dry composites were used. 25 mL of 20 (ppm) Pb (II) solutions were prepared with different range of pH values. The pH values (from 2 to 7) were adjusted by using drops of 0.1 M NaOH and 0.1 M HCl. Then, the conducted experiment was done at room temperature by shaking the solution for

2 h at 200 rpm. The effect of adsorbent dosage was investigated by different weights of the prepared PVF and PVF/MWCNTs foams (0.01, 0.04, 0.05, 0.06, 0.08, and 0.1 g), 20 mL of 20 ppm Pb (II) solutions were shaken at 200 rpm for 2 h at room temperature. To study the effect of contact time, 0.25 g of the prepared materials (PVF and PVF/ MWCNTs) in 100 mL of 20 ppm Pb<sup>2+</sup> solution was shaken at room temperature. Samples (1 mL) were taken for the analysis at the pre-determined time. The adsorption capacity ( $Q_t$ ) was calculated using equation (1):

$$Q_t = \frac{(C_0 - C_e) \times V}{W} \quad (1)$$

where:  $C_0$  is the initial concentration (mg/L),  $C_e$  is the final solution concentration (mg/L),  $V$  is the solution volume (L), and  $W$  is the weight of adsorbent material (g).

To calculate the removal percentage equation 2 was used:

$$\% \text{ of Removal} = \frac{C_0 - C_e}{C_0} \times 100 \quad (2)$$

## 2.6. Characterization techniques

FTIR spectra were recorded in the frequency range from 400-4000  $\text{cm}^{-1}$  using a VERTEX 80v (Bruker, Germany) coupled with PLATINUM ATR unit. High resolution scanning electron microscope (HRSEM), ZEISS Sigma 500 VP was used to study the morphology of the prepared foams. Energy dispersive X-ray (EDS) was conducted by EDS system attached to the same field emission of HRSEM. To measure the concentration of the lead ions, Agilent fast sequential double beam atomic absorption spectrometric system (240 FS-Agilent) equipped with air-acetylene flames was employed.

## 3. Results and discussion

### 3.1. Surface morphology

To study the structure and surface morphology of the prepared porous material, HRSEM was used. Fig. (2) shows the SEM images of (a) PVF foam and (b) PVF/MWCNTs. From Fig. 2 (a), one can observe the spongy structure of the prepared PVF foam matrix. Also the foam exhibits an open-cell interconnecting macro-porous network structure [27]. After the addition of MWCNTs into the PVF matrix, Fig 2(b), the surface roughness and porosity of the PVF foam significantly changed. One can clearly observe the presence of MWCNTs bundles fill and connecting the PVF porous. Obviously, the addition of MWCNTs increased the surface roughness and changed the regular macro-porous network structure to opened lamellar structure [28]. After the adsorption of Pb (II) onto the composite, small crystals of lead aggregations appeared on the surface

of PVF/ MWCNTs foam [Fig. 2(c)]. In addition, EDX analysis confirmed the adsorption of Pb ions on the surface of PVF/ MWCNTs foam [see Fig. 3]. Moreover, elemental mapping was used to investigate the distribution of Pb (II) on surface of the PVF/ MWCNTs foam as can be seen in Fig. 2(d). Also, the mapping image showed the lead ions are distributed homogeneously on the foam's surface. This can be owing to that the MWCNTs are homogeneously distributed inside the PVF foam matrix. In addition, the weight percentage of Pb over the surface was equal to about 2.5% as calculated from the EDX results.

### 3.2. FTIR

Fig.4 (a)-(c) depicts the FTIR spectra for MWCNTs, PVF, and PVF/MWCNTs foams, respectively. For the MWCNTs [Fig. 4 (a)], the broad band centered at 3340  $\text{cm}^{-1}$  is related to the O-H stretching mode. The presence of absorption bands at  $\approx 2848$ , 2920, and 2960  $\text{cm}^{-1}$  are due to the presence of C-H<sub>n</sub> groups. The band appeared at  $\approx 1727$   $\text{cm}^{-1}$  is related to C=O stretching vibration. The C=C stretching mode band is centered at 1650  $\text{cm}^{-1}$ . The band located at  $\approx 1060$   $\text{cm}^{-1}$  could be ascribed to the C-O stretching vibration mode [29]. For blank PVF foam (Fig. 4(b)), the absorption band at 3340  $\text{cm}^{-1}$  is characteristic to the O-H stretching mode. The CH<sub>2</sub> symmetric stretching mode can be observed at four bands at 2943, 2910, 2857, and 2777  $\text{cm}^{-1}$  [30–32]. The O–H bending vibration band appeared at 1642  $\text{cm}^{-1}$ . The bands located at 1447, 1426, 1398, and 1349  $\text{cm}^{-1}$  are attributed to the C-H bending mode. The C-O-C stretching mode appeared at 1008  $\text{cm}^{-1}$ . The presence of the C-O-C-O-C stretching vibrations resulted in the appearance of bands located at 1175, 1126 and 1062  $\text{cm}^{-1}$  [27,33]. For the PVF/ MWCNTs foam

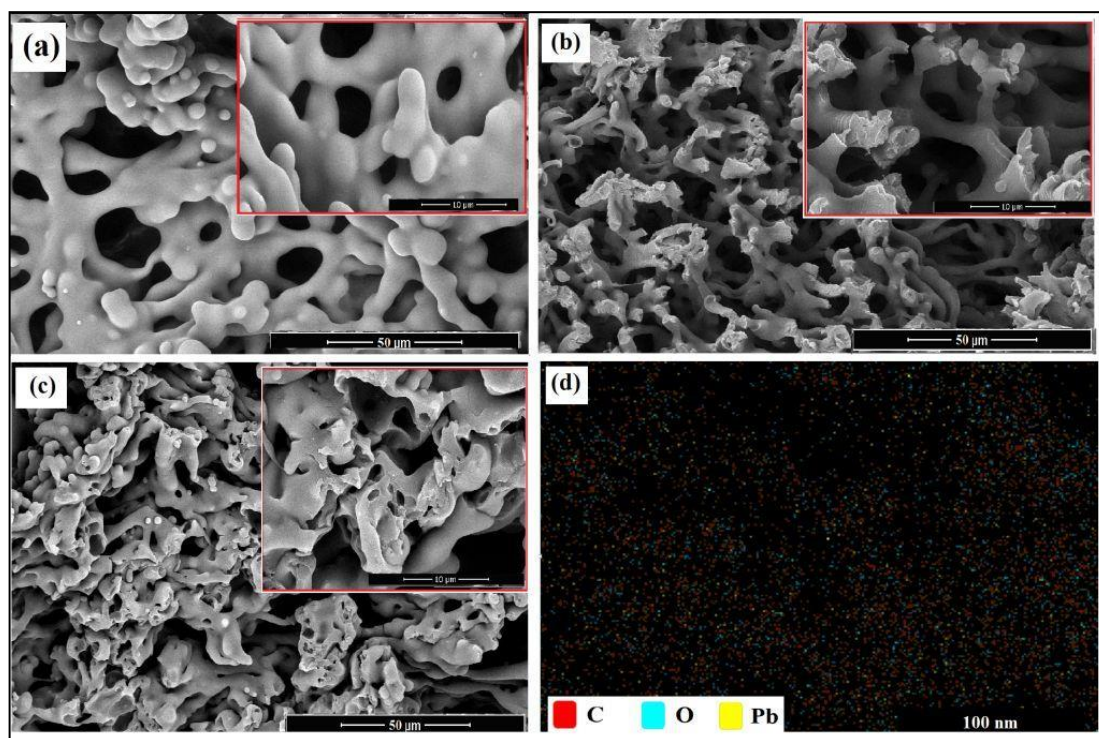


Figure 2: HRSEM image of (a) Blank PVF foam, (b) PVF/MWCNTs composite, (c) PVF/MWCNTs foam after Pb adsorption, and (d) elemental mapping of the PVF/MWCNTs foam loaded with Lead crystals

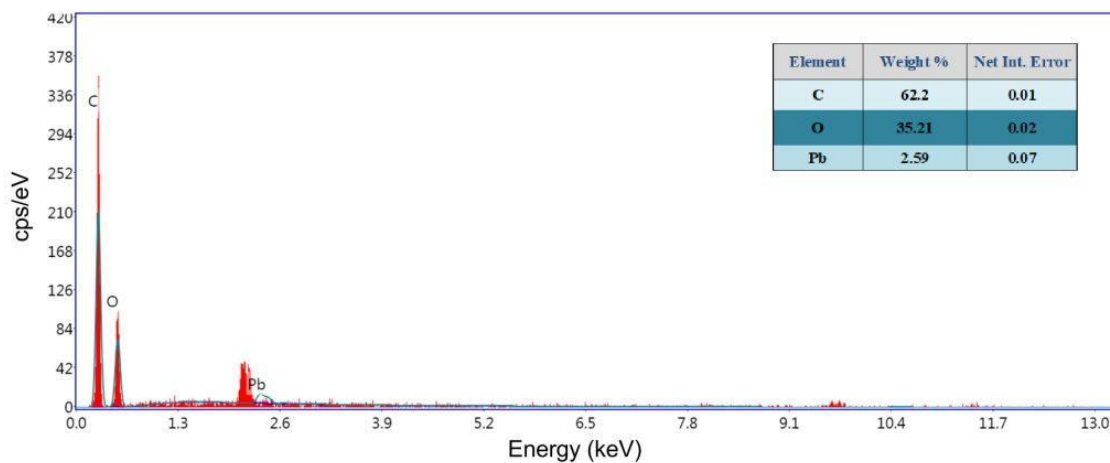


Figure 3: The energy dispersive X-ray (EDX) elemental analysis of PVF/MWCNTs foam loaded with Lead crystals.

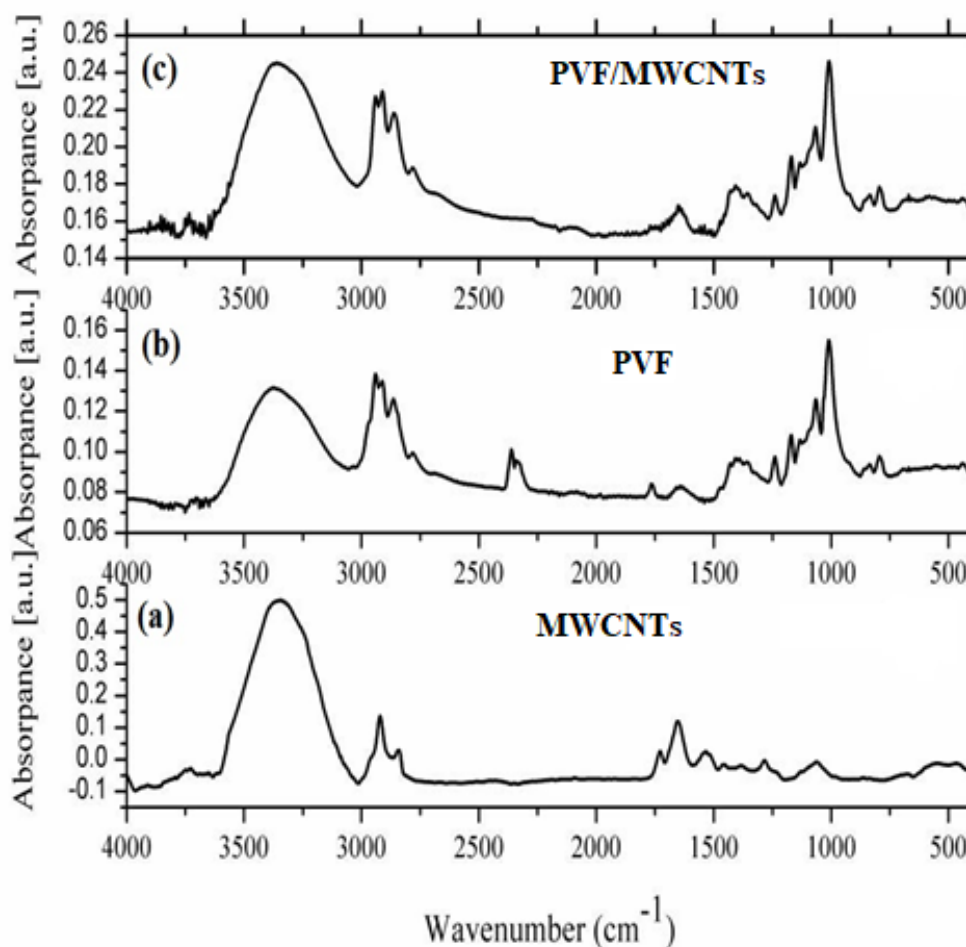


Figure 4: FTIR spectra of (a) as grown MWCNTs powder, (b) blank PVF foam, and (c) PVF/MWCNTs composite in the frequency range 400 - 4000  $\text{cm}^{-1}$ .

(Fig. 4-c), the presence of O-H groups from the MWCNTs resulted in increasing the total amount of free O-H groups in the PVF matrix, accordingly the intensity of the band related to O-H stretching mode was increased. The other main peaks characteristic to blank PVF foam can be observed clearly with no major changes indicating that carbon nano tubes were attached to the foam matrix via van der Waals forces [33].

### 3.4. Factors affecting the ( $Q_t$ ) adsorption capacity

#### 3.4.1. pH effect

The adsorption capacity of the metal ions in the solution is highly dependent on the pH value. The competition occurs between the  $\text{H}^+$  on the adsorbent

active sites and the Pb (II) ions in the solution are affected by the solution acidity.

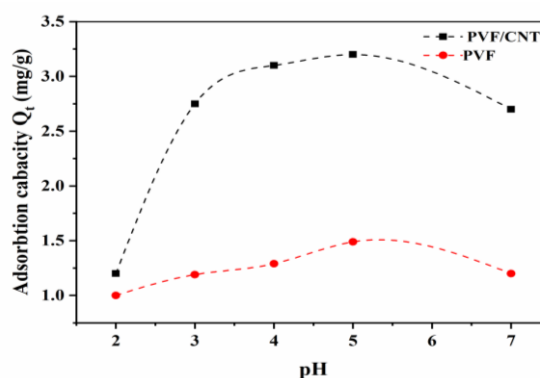


Figure 5: Influence of pH value on the adsorption capacity of Lead ions over blank PVF and PVF/MWCNTs foam. The other parameter set at 0.04 g dose, 25 mL of 20 (ppm) Pb (II) solutions.

Figure 5 depicts the relation between the adsorption capacity ( $Q_t$ ) and the pH value of the solution. The  $Q_t$  of Pb (II) was increased by increasing the pH value till it reached a maximum at around pH 4-5. After that the  $Q_t$  value started to decrease due to the effect of the precipitation of lead hydroxide when the pH exceeds to 7 [34,35].

### 3.4.2. Initial adsorbent dosage

The adsorbent dosage is one of the important factors which affecting the adsorption behavior. Figure 6 shows the relation between the initial adsorbent dosage for PVF and PVF/ MWCNTs foams (expressed in grams) and the total adsorption capacity. It can be noted that, at pH 5 the total  $Q_t$  value was enhanced by increasing the initial dosage. The maximum  $Q_t$  was obtained at dosage 0.05 g (the equilibrium point) for both tested samples. After that, the  $Q_t$  value decreased with increasing sorbent dosage. This could be explained as follows: by increasing the total number of available free adsorbing sites on the sorbent, the total adsorbed lead ions per unit mass of sorbent decreases, accordingly the total  $Q_t$  value obviously decreased [36]. Furthermore, the adsorbed Pb (II) onto the material surface might blocked the other lead ions from reaching the internal pores of adsorbent, leading to a decrease in the total adsorption capacity [37].

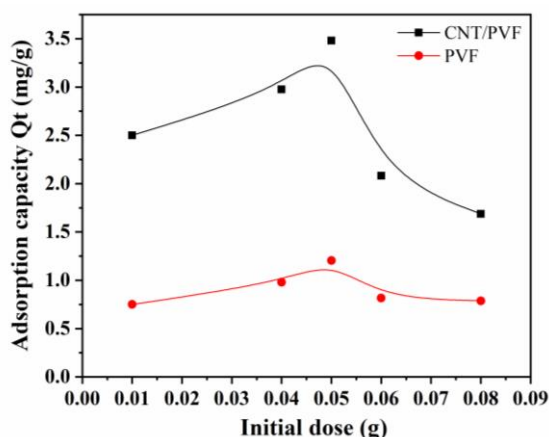


Figure 6: Effect of the adsorbent weight on the adsorption capacity of Pb (II) ions onto blank PVF and PVF/MWCNTs foam (at pH 5, and 20 ml of 20 ppm lead solution).

### 3.4.3. Contact time

The effect of contact time on the adsorption of Pb (II) from aqueous solution onto PVF and PVF/ MWCNTs foams is presented in Figure 7. The  $Q_t$  was rapidly increased by increasing the contact time. The maximum  $Q_t$  value is reached at 40 and 60 min for PVF, PVF/ MWCNTs, respectively, all other parameters were kept at optimum conditions (pH=5, dose 0.05g). The equilibrium between Pb (II) and adsorbent active sites at such time was achieved and after that no obvious change in the value of adsorption capacity was observed.

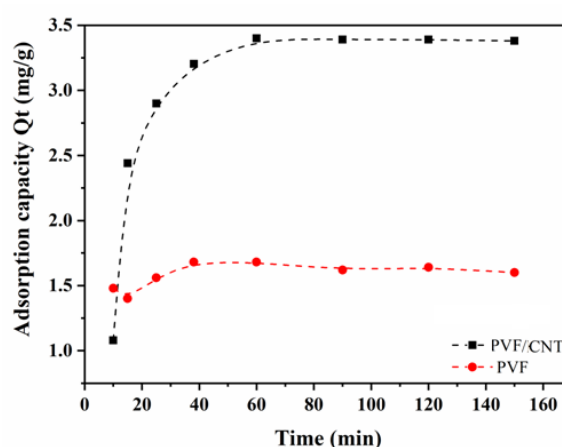


Figure 7: Effect of the contact time on the adsorption capacity of Pb (II) ions onto blank PVF and PVF/ MWCNTs foam (at pH 5, and 0.25 g sorbent in 100 mL of 20 ppm Pb<sup>2+</sup> solution).

## 4. Adsorption kinetics

Different kinetic models can be used to examine the rate of the adsorption process and the rate-controlling step in liquid-phase systems such as: the intra-particle diffusion model, pseudo-first-order, and pseudo- second-order model [38]. Regarding the correlation coefficient ( $R^2$ ) values of the linear regression, the best-fit model is selected. If the experimental adsorption capacities  $q_e$  (from the batch experiment results) is in compliance with the theoretical calculated data, therefore, the selected model would be the best one describing the overall adsorption process [37,39].

### 4.1. Pseudo first-order kinetic model

According to this model, the adsorption rate is determined based on the available binding sites on the adsorbent surface. The linear form of the pseudo-first-order model is described by Equation (3):

$$\log [q_e - q_t] = \log [q_e] - \left[ \frac{K_1}{2.303} \right] t \quad (3)$$

where,  $q_e$  and  $q_t$  are the adsorption value of Pb (II) at equilibrium and pre-determined time  $t$  (mg/g), respectively.  $K_1$  is the pseudo-first-order kinetic model rate constant ( $\text{min}^{-1}$ ). According to equation 3, the slope of the straight line between  $\log (q_e - q_t)$  against  $(t)$  gives  $K_1$ , while the y-intercept is the value of  $q_e$  (Figure 8-a).

#### 4.2. Pseudo second-order kinetic model:

This model assumes that the rate of adsorption is dependent on the square of the number of free sites. Equation (4) describes the pseudo second-order kinetic model:

$$\frac{t}{q_t} = \frac{1}{K_2 \times q_e^2} + \frac{t}{q_e} \quad (4)$$

**Table 1:** The kinetic models calculation for Pb (II) ions removal by PVF and PVF/ MWCNTs.

Adsorbent	$q_e$ (Exp) (mg/g)	Pseudo first-order			Pseudo second-order		
		$q_e$ (mg/g)	$k_1$ ( $\text{min}^{-1}$ )	$R^2$	$q_e$ (mg/g)	$k_2$ ( $\text{min}^{-1}$ )	$R^2$
PVF	1.6	2.9	0.05	0.944	1.8	0.11	0.998
PVF/MWCNTs	3.12	1.3	0.059	0.965	3.2	0.081	0.999

#### 4.3. Intra-particle diffusion model

This model is described by a liner relationship between the specific sorption ( $q_t$ ) and the square root of time as:

$$q_t = K_{int} \times t^{1/2} \quad (5)$$

As suggested by Weber and Morris, the diffusion mechanism of the process is described by a

where,  $q_e$  and  $q_t$  (mg/g) are the adsorption value of lead ions at equilibrium and time  $t$ , respectively.  $K_2$  ( $\text{min}^{-1}$ ) is the reaction rate constant of the pseudo-second-order model.  $t/q_t$  versus  $t$  was plotted then  $q_e$  and  $K_2$  were calculated (Figure 8-b). The summarized results of pseudo first-order, and pseudo second-order kinetic models  $K_1$ ,  $K_2$ ,  $q_e$  (theoretical),  $q_e$  (experimental) and  $R^2$  values are listed in Table 1. The adsorption mechanism of lead ions from an aqueous solution onto the prepared foam obeys the pseudo-second-order kinetic model with good values of the correlation coefficient ( $R^2$ ) 0.998 and 0.999 for PVF and PVF/ MWCNTs, respectively. The adsorption values of Pb (II) at equilibrium ( $q_e$ ) for PVF and PVF/ MWCNTs were 1.6 and 3.12 (mg/g), respectively. Therefore, the rate-limiting step of this adsorption process mechanism might be chemisorption process [40].

linear plot of  $q_t$  against  $t^{1/2}$ . If the plotted graph was a straight line which passes through the origin point, so the adsorption process has one rate-limiting step [41]. However, McKay and Allen suggested that if the graph of  $q_t$  vs.  $t^{1/2}$  divided into more than one sections, so there are many steps occurs [42].

Figure 9 reveals the Intra-particle diffusion model graph for both PVF and PVF/ MWCNTs

foams. For the PVF foam, the relation exhibit one liner plot indicating that the diffusion process of metal ions into the pours material occurred in one rate-limiting step.

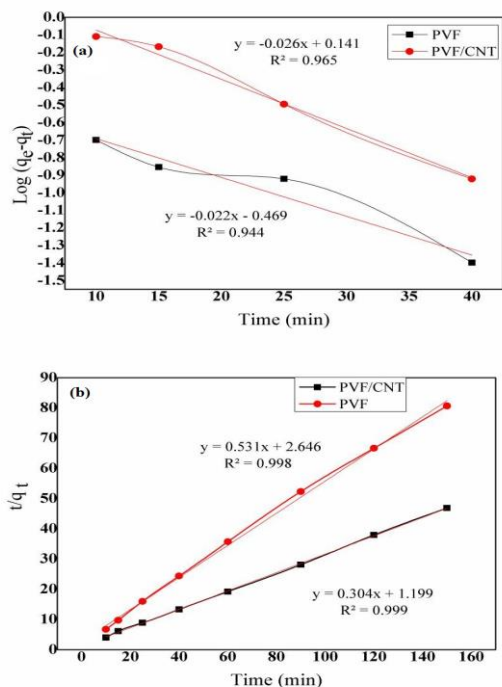


Figure 8: Adsorption kinetics fitting data of Pb onto blank PVF and PVF/CNT composite, (a) pseudo-first-order kinetic model, and (b) pseudo-second-order kinetic model

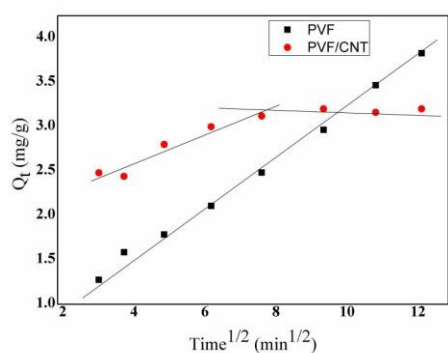


Figure 9: Intra-particle diffusion model graph for both PVF and PVF/CNT.

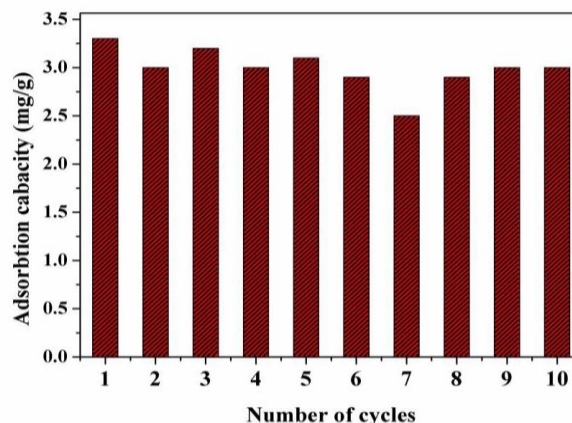


Figure 10: Effect of regeneration on the maximum adsorption capacity of the PVF/CNT foam using, 0.05g dose, pH=5, and 60 min contact time.

In case of the PVF/ MWCNTs foam, two well defined linear sections were obtained indicating that the diffusion process occurred in two stages [42]. At the first, rapid diffusion of lead ions from the aqueous phase to the adsorbent outer-surface until reached to saturation. After that, a second stage occurred due to a slow adsorption into the porous structure of the adsorbents [21].

## 5. Desorption and reusability

Long-term stability of the prepared PVF/ MWCNTs material was investigated by successfully desorption of the adsorbed lead ions. Thus, the PVF/ MWCNTs can be effectively used repeatedly in heavy metal removal processes. A solution of 10%  $\text{H}_2\text{SO}_4$  was used to desorb the  $\text{Pb}^{2+}$  and re-generates the free active sites. The prepared composite shows an excellent desorption-adsorption property for more than 10 cycles which will effectively reduce the overall cost for the removal process [see Fig. 10].

## 6. Conclusion

A novel highly mechanical and chemical stable sorbent based on PVF/ MWCNTs macro-porous sponges was successfully prepared via *in-situ* traditional acetylation reaction of polyvinyl formaldehyde. The sorbent molecular structure was characterized by FT-IR spectroscopy. Scanning

electron microscopy was used to study the morphology characteristics of the prepared composite and EDX elemental analysis. The kinetic models were discussed for the adsorption mechanisms and the results reveal that the prepared sponge adsorption mechanism was best fitted with the pseudo second-order kinetic model with  $R^2$  value 0.9959, and the rate limiting step is chemisorption in nature. Moreover, the prepared composite exhibits great desorption-adsorption ability for up to 10 cycles with almost the same removal efficiency. Therefore, the developed PVF/ MWCNTs foam matrix is suggested to be an effective eco-friendly sorbent for water treatment systems.

### References

- [1] S. Babel, T.A. Kurniawan, Low-cost adsorbents for heavy metals uptake from contaminated water: a review, *J. Hazard. Mater.* 97 (2003) 219–243.
- [2] R. Khlifi, A. Hamza-Chaffai, Head and neck cancer due to heavy metal exposure via tobacco smoking and professional exposure: a review, *Toxicol. Appl. Pharmacol.* 248 (2010) 71–88.
- [3] C.B. Ernhart, A critical review of low-level prenatal lead exposure in the human: 1. Effects on the fetus and newborn, *Reprod. Toxicol.* 6 (1992) 9–19.
- [4] A.S. Mahmoud, N. Youssef, A.M. Osama, M. Selim, Removal of Lead Ions from Industrial Wastewater Using Magnetite Loaded on Silica Support, *Egypt. J. Chem.* 62 (2019) 2163–2173.
- [5] C.K. Singh, J.N. Sahu, K.K. Mahalik, C.R. Mohanty, B.R. Mohan, B.C. Meikap, Studies on the removal of Pb (II) from wastewater by activated carbon developed from Tamarind wood activated with sulphuric acid, *J. Hazard. Mater.* 153 (2008) 221–228.
- [6] V.K. Gupta, O. Moradi, I. Tyagi, S. Agarwal, H. Sadegh, R. Shahryari-Ghoshekandi, A.S.H. Makhlof, M. Goodarzi, A. Garshasbi, Study on the removal of heavy metal ions from industry waste by carbon nanotubes: effect of the surface modification: a review, *Crit. Rev. Environ. Sci. Technol.* 46 (2016) 93–118.
- [7] S. Farag, H.M. Ibrahim, A. Amr, M.S. Asker, A. El-shafie, Preparation and characterization of ion exchanger based on bacterial cellulose for heavy metal cation removal, *Egypt. J. Chem.* 63 (2020) 23–24.
- [8] N. Ammar, A. Fahmy, S. Kanawy Ibrahim, E.M.A. Hamzawy, M. El-Khateeb, Wollastonite ceramic/CuO nano-Composite For cadmium ions removal from waste water, *Egypt. J. Chem.* 60 (2017) 817–823.
- [9] M. Alshabanat, Removal of heavy metal ions using polystyrene nanocomposite thin films, *Egypt. J. Chem.* 62 (2019) 149–156.
- [10] A. Fahmy, A. Elzaref, H. Youssef, H. Shehata, M. Wassel, J. Friedrich, F. Poncin-Epaillard, D. Debarnot, Plasma O<sub>2</sub> modifies the structure of synthetic zeolite-A to improve the removal of cadmium ions from aqueous solutions, *Turkish J. Chem.* 43 (2019) 172–184. <https://doi.org/10.3906/kim-1808-14>.
- [11] F. Ekmekyapar, A. Aslan, Y.K. Bayhan, A. Cakici, Biosorption of copper (II) by nonliving lichen biomass of *Cladonia rangiformis* hoffm., *J. Hazard. Mater.* 137 (2006) 293–298.
- [12] F. Ge, M.-M. Li, H. Ye, B.-X. Zhao, Effective removal of heavy metal ions Cd<sup>2+</sup>, Zn<sup>2+</sup>, Pb<sup>2+</sup>, Cu<sup>2+</sup> from aqueous solution by polymer-modified magnetic nanoparticles, *J. Hazard. Mater.* 211

- (2012) 366–372.
- [13] P. Thamilarasu, K. Karunakaran, Kinetic, equilibrium and thermodynamic studies on removal of Cr (VI) by activated carbon prepared from *Ricinus communis* seed shell, *Can. J. Chem. Eng.* 91 (2013) 9–18.
- [14] F. Najafi, O. Moradi, M. Rajabi, M. Asif, I. Tyagi, S. Agarwal, V.K. Gupta, Thermodynamics of the adsorption of nickel ions from aqueous phase using graphene oxide and glycine functionalized graphene oxide, *J. Mol. Liq.* 208 (2015) 106–113.
- [15] Z. Çelik, M. Gülfen, A.O. Aydın, Synthesis of a novel dithiooxamide–formaldehyde resin and its application to the adsorption and separation of silver ions, *J. Hazard. Mater.* 174 (2010) 556–562.
- [16] Y.-H. Li, S. Wang, J. Wei, X. Zhang, C. Xu, Z. Luan, D. Wu, B. Wei, Lead adsorption on carbon nanotubes, *Chem. Phys. Lett.* 357 (2002) 263–266.
- [17] D. Xu, X. Tan, C. Chen, X. Wang, Removal of Pb (II) from aqueous solution by oxidized multiwalled carbon nanotubes, *J. Hazard. Mater.* 154 (2008) 407–416.
- [18] M. Ghaedi, M. Montazerzohori, N. Rahimi, M.N. Baysreh, Chemically modified carbon nanotubes as efficient and selective sorbent for enrichment of trace amount of some metal ions, *J. Ind. Eng. Chem.* 19 (2013) 1477–1482.
- [19] H. Tavallali, H. Malekzadeh, M.A. Karimi, M. Payehghadr, G. Deilamy-Rad, M. Tabandeh, Chemically modified multiwalled carbon nanotubes as efficient and selective sorbent for separation and preconcentration of trace amount of Co(II), Cd(II), Pb(II), and Pd(II), *Arab. J. Chem.* 12 (2019) 1487–1495.
- <https://doi.org/10.1016/j.arabjc.2014.10.034>.
- [20] L. Torkian, M.M. Amini, T. Gorji, O. Sadeghi, A simple, rapid and sensitive method based on modified multiwalled carbon nanotube for preconcentration and determination of lead ions in aqueous media in natural pHs, *Arab. J. Chem.* 12 (2019) 1315–1321.
- <https://doi.org/10.1016/j.arabjc.2014.10.041>.
- [21] M. Jahangiri, F. Kiani, H. Tahermansouri, A. Rajabalinezhad, The removal of lead ions from aqueous solutions by modified multi-walled carbon nanotubes with 1-isatin-3-thiosemicarbazone, *J. Mol. Liq.* 212 (2015) 219–226.
- <https://doi.org/10.1016/j.molliq.2015.09.010>.
- [22] M.A. Tofighy, T. Mohammadi, Adsorption of divalent heavy metal ions from water using carbon nanotube sheets, *J. Hazard. Mater.* 185 (2011) 140–147. <https://doi.org/10.1016/j.jhazmat.2010.09.008>.
- [23] M.A. Tofighy, T. Mohammadi, Salty water desalination using carbon nanotube sheets, *Desalination.* 258 (2010) 182–186.
- [24] A. Abouelsayed, B. Anis, S. Hassaballa, A.S.G. Khalil, U.M. Rashed, K.A. Eid, E. Al-Ashkar, W. [El hotaby], Preparation, characterization, Raman, and terahertz spectroscopy study on carbon nanotubes, graphene nano-sheets, and onion like carbon materials, *Mater. Chem. Phys.* 189 (2017) 127–135.
- <https://doi.org/https://doi.org/10.1016/j.matchemphys.2016.12.065>.
- [25] B. Anis, H. El Fllah, T. Ismail, W.M. Fathallah, A.S.G. Khalil, O.M. Hemedat, Y.A. Badr, Preparation, characterization, and thermal conductivity of polyvinyl-formaldehyde/MWCNTs foam: A low cost heat sink substrate, *J. Mater. Res.*

- Technol. (2020) 1–12. <https://doi.org/10.1016/j.jmrt.2020.01.044>.
- [26] Y. Pan, C. Peng, W. Wang, K. Shi, Z. Liu, X. Ji, Preparation and absorption behavior to organic pollutants of macroporous hydrophobic polyvinyl alcohol-formaldehyde sponges, *RSC Adv.* 4 (2014) 35620–35628. <https://doi.org/10.1039/c4ra03278k>.
- [27] B. Xue, R. Li, J. Deng, J. Zhang, Sound Absorption Properties of Microporous Poly(vinyl formal) Foams Prepared by a Two-Step Acetalization Method, *Ind. Eng. Chem. Res.* 55 (2016) 3982–3989. <https://doi.org/10.1021/acs.iecr.6b00127>.
- [28] A.A. Artyukhov, M.I. Shtilman, A.N. Kuskov, L.I. Pashkova, A.M. Tsatsakis, A.K. Rizos, Polyvinyl alcohol cross-linked macroporous polymeric hydrogels: Structure formation and regularity investigation, *J. Non. Cryst. Solids.* 357 (2011) 700–706.
- [29] B. Anis, A.M. Mostafa, Z.A. El Sayed, A.S.G. Khalil, A. Abouelsayed, Preparation of highly conductive, transparent, and flexible graphene/silver nanowires substrates using non-thermal laser photoreduction, *Opt. Laser Technol.* 103 (2018) 367–372.
- [30] P. Chetri, N.N. Dass, Preparation of poly (vinyl formal) of high acetalization, *Polymer (Guildf).* 38 (1997) 3951–3956.
- [31] B. Xue, J. Deng, J. Zhang, Multiporous open-cell poly (vinyl formal) foams for sound absorption, *RSC Adv.* 6 (2016) 7653–7660.
- [32] A. Fahmy, D. Debarnot, J. Friedrich, Influence of water addition on the structure of plasma-deposited allyl alcohol polymer films, *J. Adhes.* Sci. Technol. 29 (2015) 965–980.
- [33] S. Chakravarty, A. Datta, N. Sen Sarma, An electrical solid-state sulphur dioxide vapour sensor based on a polyvinyl alcohol formaldehyde composite, *J. Mater. Chem. C.* 5 (2017) 2871–2882.
- [34] X.-H. Zhao, F.-P. Jiao, J.-G. Yu, Y. Xi, X.-Y. Jiang, X.-Q. Chen, Removal of Cu(II) from aqueous solutions by tartaric acid modified multi-walled carbon nanotubes, *Colloids Surfaces A Physicochem. Eng. Asp.* 476 (2015) 35–41. <https://doi.org/10.1016/j.colsurfa.2015.03.016>.
- [35] N.A. Kabbashi, M.A. Atieh, A. Al-Mamun, M.E.S. Mirghami, M.D.Z. Alam, N. Yahya, Kinetic adsorption of application of carbon nanotubes for Pb (II) removal from aqueous solution, *J. Environ. Sci.* 21 (2009) 539–544.
- [36] H. Aydın, Y. Bulut, Ç. Yerlikaya, Removal of copper (II) from aqueous solution by adsorption onto low-cost adsorbents, *J. Environ. Manage.* 87 (2008) 37–45.
- [37] N. Kannan, T. Veemaraj, Removal of Lead (II) Ions by adsorption onto bamboo dust and commercial activated Carbons-A comparative study, *J. Chem.* 6 (2009) 247–256.
- [38] M.M. Rao, G.P.C. Rao, K. Sessaiah, N. V Choudary, M.C. Wang, Activated carbon from Ceiba pentandra hulls, an agricultural waste, as an adsorbent in the removal of lead and zinc from aqueous solutions, *Waste Manag.* 28 (2008) 849–858.
- [39] A. Fahmy, A. El-Zomrawy, A.M. Saeed, A.Z. Sayed, M.A.E. El-Arab, H. Shehata, J. Friedrich, Degradation of organic dye using plasma

- discharge: optimization, pH and energy, Plasma Res. Express. 2 (2020) 15009.
- [40] H. Ys, G. McKay, H. Ys, G. McKay, Pseudo-second order model for sorption processes, Process Biochem. 34 (1999) 451–465.
- [41] W.J. Weber, J.C. Morris, Kinetics of adsorption on carbon from solution, J. Sanit. Eng. Div. 89 (1963) 31–60.
- [42] G. McKay, S.J. Allen, Surface mass transfer processes using peat as an adsorbent for dyestuffs, Can. J. Chem. Eng. 58 (1980) 521–526.